RSC Advances

PAPER

View Article Online
View Journal | View Issue

Cite this: *RSC Adv.*, 2014, **4**, 22926

Hybrid poly(3-hexyl thiophene)–TiO_2 nanorod oxygen sensor†

Che-Pu Hsu,‡[a] Tsung-Wei Zeng,‡[a] Ming-Chung Wu,[b] Yu-Chieh Tu,[a] Hsueh-Chung Liao[a] and Wei-Fang Su*[a]

Received 9th March 2014
Accepted 12th May 2014

DOI: 10.1039/c4ra02058h

www.rsc.org/advances

Conjugated polymers are promising materials for oxygen sensing owing to their specific interaction with oxygen molecules and also advantages of low cost, easy processing and room temperature operation. The present work for the first time demonstrates an oxygen sensing material of poly(3-hexylethiophene) (P3HT)–TiO_2 nanorod hybrid thin film which reveals considerable improvement of sensing response as compared to the pristine P3HT film. The effects of hybrid composition and film thickness on sensing performance were systematically investigated. Kelvin probe force microscopy (KPFM) was employed to understand the mechanism of oxygen sensing including the control of surface morphologies and electronic properties by TiO_2 incorporation. The hybrid material developed in this study is helpful in the advancement of room temperature oxygen sensing technology.

Introduction

Oxygen sensing devices are extremely important in daily life, manufacturing, research and development. Most of the commercial available oxygen sensors are made from metal-oxide material such as ZrO_2, TiO_2, Ga_2O_3, *etc.* which are high cost and have to operate at high temperature.[1–3] Conjugated polymers are promising materials for gas sensing since they provide many advantages such as low cost, solution processing, room temperature operation, *etc.* Previous literatures have demonstrated their capability in gas sensing through tracing the variation of gas-sensitive properties, *e.g.* conductivity, work function and optical absorption spectra.[4] The variation of conductivity can be easily detected and employed in electronic devices which is ideal for gas sensing device. Among the conjugated polymers, polythiophene and its derivatives have attracted considerable attention due to their good environmental and thermal stability.[5] Polythiophenes have been used as sensing materials for different gases and vapors such as oxygen,[6,7] NO_x[8,9] and other volatile compounds.[5,10–12] The study of reaction mechanism between P3HT and oxygen revealed that oxygen is physically absorbed on P3HT as dopant which is reversible.[6,7,13]

In order to improve the sensing performance of conjugated polymer, adding inorganics into polymers, so called organic–inorganic hybrid materials, have been investigated recently for gas sensor applications.[14,15] By combing distinct properties of two materials, the sensitivity and selectivity for various gases have shown enhancement. Nanostructured inorganic materials have been fabricated into ultrasensitive sensors.[16–19] In this work, inorganic TiO_2 nanocrystals were incorporated into the conjugated polymer of poly(3-hexylthiophene) (P3HT). Such composites have been extensively applied in a variety of applications,[20–23] however, this is the first time we show that such composites can be employed in a room temperature operated oxygen sensing device. By controlling the nano- and micro-morphology of hybrid films, so the sensing response toward oxygen has been improved. The conductivity variation of the film was used as indication for detecting oxygen. The sensing performances were investigated with respect to different P3HT–TiO_2 hybrid ratios and film thickness. KPFM technique was utilized to understand the mechanism of improved sensing response by TiO_2 incorporation. Our study demonstrates a newly developed hybrid material for enhancing the performance of oxygen sensing at room temperature.

Experimental details

The conducting polymer P3HT with molecular weight of 62 kDa was synthesized in our laboratory according to the literature.[24] The precursor of P3HT is 2,5-dibromo-3-hexylthiophene, and the addictions are *tert*-butylmagnesium chloride and Ni(dppp)Cl_2. The anatase TiO_2 nanorods (~5 nm × 30 nm) were synthesized *via* a low-temperature (~70 °C) sol–gel method.[25,26] The precursor of TiO_2 is titanium isopropoxide and the surfactant is oleic acid. The as synthesized TiO_2 nanorods were then modified by small molecules pyridine to partially remove

[a]*Department of Materials Science and Engineering, National Taiwan University, Taipei 106-17, Taiwan. E-mail: suwf@ntu.edu.tw*

[b]*Department of Chemical and Materials Engineering, Chang Gung University, Taoyuan 333-02, Taiwan. E-mail: mingchungwu@mail.cgu.edu.tw*

† Electronic supplementary information (ESI) available: The response time and recovery time of the oxygen sensor. See DOI: 10.1039/c4ra02058h

‡ These authors contributed equally to the work.

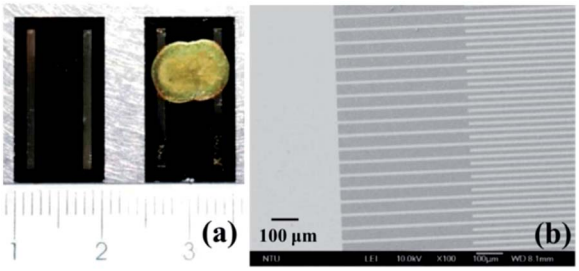

Fig. 1 (a) The photo of accomplished oxygen sensor device and (b) SEM image of bar structure Au electrodes.

the insulating surface ligand oleic acid.[27,28] The SiO_2 nanocrystals were purchased from Nissan Chemical (20–30 nm, MA-ST-M, 40 wt% solid content) and used as received. The P3HT was dissolved in chloroform with a concentration of 30 mg ml^{-1}, and the TiO_2 solution with a concentration of 10 mg ml^{-1} were prepared by using co-solvents of pyridine–dichloromethane–chloroform with volume ratio of 1 : 2 : 3. Lastly, the P3HT–TiO_2 nanorods hybrid solutions with different TiO_2 concentration were stirred at 40 °C overnight in the glove box. We use oxidized silicon wafer as substrate. The thickness of surface silicon oxide is around 1000 nm, and the thickness of silicon wafer base is around 1 mm. The pristine P3HT thin film and hybrid films of P3HT–TiO_2 were deposited on the substrates, with an Au electrode of which interdigitated width of 15 μm and interval of 10 μm, by drop casting or spin casting process at 4000 r.p.m. for 1 min in the glove box (Fig. 1). The thickness of the drop casted films and spin casted films were around 10 μm and 200 nm respectively. The sensor devices were placed in a sealed chamber with controlled feed of oxygen gas and nitrogen gas and the *I–V* curves were recorded by picoammeter (Keithley, model 6487) at room temperature. During the sensing procedure, the oxygen gas was fed into the chamber for 4 minutes then followed by nitrogen feeding for 36 minutes. Such procedure was repeated for 4 times with simultaneous record of *I–V* curves for obtaining resistance *R* (*i.e.* *I*/*V*). The surface topography and surface potential of sample films were mapped by Kelvin probe force microscope (Veeco instruments Multimode AFM with an extender electronics module). Scanning was performed in the lift mode with height of 20 nm by silicon cantilevers with Pt/Ir surface coating.[29] The SEM cross-sectional images were obtained by utilizing JOEL JSM-6700F field emission scanning electron microscope at acceleration voltage of 10.0 kV.

Results and discussion

We used a simple expression of R_0/R for clearly presenting the sensing responses of our devices, where R is the resistance of thin film device after oxygen exposure and R_0 is the initial resistance before oxygen exposure. Such simple definition was also employed in other literatures of sensor research, *e.g.* R_d/R_h, R_{air}/R_{gas}, R_{gas}/R_{air}, V_g/V_a, I/I_0, I_0/I, *etc.*[30–35] The definition takes the advantage of easier signal processing for the further on industrial applications. Fig. 2 shows the sensing response of drop

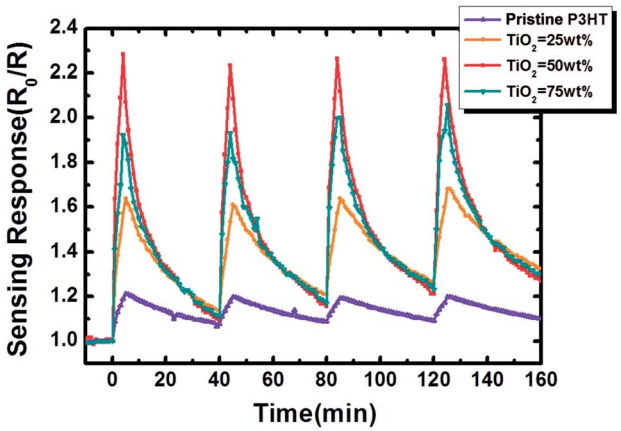

Fig. 2 Sensing response (R_0/R) of drop casted P3HT film and P3HT–TiO_2 hybrid films with different TiO_2 loading concentrations (*i.e.* 0 wt%, 25 wt%, 50 wt%, and 75 wt%) during sensing procedure.

casted pristine P3HT film and P3HT–TiO_2 hybrid films with different TiO_2 loading concentration. The R_0 values of P3HT–TiO_2 hybrid films with different TiO_2 loading concentration, *i.e.* 0 wt%, 25 wt%, 50 wt% and 75 wt% are 4.0×10^6 Ω, 5.6×10^7 Ω, 1.9×10^8 Ω and 9.2×10^8 Ω respectively. All the sample films showed an instant response upon oxygen exposure (jump of R_0/R values), which indicates the enhanced conductivity of the sample films. This can be attributed to the increasing carriers concentration resulted from oxygen doping.[6,13] Namely, the weakly chemical bounded donor–acceptor complexes or charge transfer complexes are formed by the interaction between P3HT and oxygen molecule. Namely, the interaction between a molecule with low ionization potential (an electron donor, P3HT) and a molecule with relatively high electron affinity (an electron acceptor, oxygen molecule) can lead to a weakly bound donor–acceptor complex or charge transfer complex (CTC). Evidences for this reversible process (adsorption and desorption) have been shown in the literature by using UV-vis absorption and electron paramagnetic resonance (EPR) spectroscopic analyses[6,7] Additionally, introducing TiO_2 nanorods into P3HT led to significantly increased sensing response by around 2 times as shown in Fig. 2. Among the hybrid films, the loading concentration of 50 wt% reveals the highest sensing response as compared with other blending ratios.

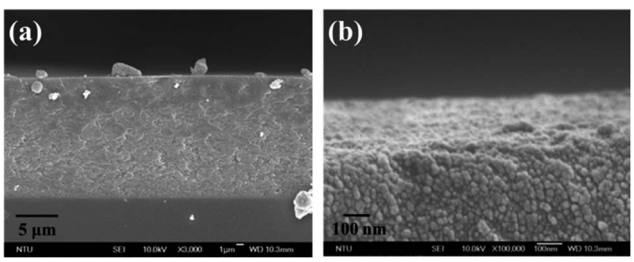

Fig. 3 Cross-sectional SEM images of hybrid film containing 50 wt% TiO_2 nanorods show (a) the film thickness and (b) the morphology of hybrid film with several tens of nanometer nano-domain.

The cross-sectional SEM images of hybrid film with 50 wt% TiO_2 nanorods are shown in Fig. 3. The hybrid film thickness is about 15 μm (Fig. 3(a)), and the blended P3HT : –TiO_2 nanorods hybrid material in spherical shape in the size of several tens of nanometer is observed (Fig. 3(b)).

For clarifying the effect of TiO_2 nanorods in oxygen sensing, we compared the sensing response of three types of devices fabricated from three different films sandwiched between glass substrates and interdigitated Au electrodes. They are (1) a single layer of pristine P3HT film with thickness of 100 nm, (2) bi-layers of pristine P3HT (~100 nm) film on top of a TiO_2 film (~100 nm, deposited from TiO_2 nanorods solution), and (3) bi-layers of pristine P3HT (~100 nm) film on top of a SiO_2 film (~100 nm). All the layers were deposited by spin coating. The sensitivities of the three devices are shown in Fig. 4. As compared with single layer P3HT, including the TiO_2 layer considerably improves the sensing response, while the P3HT–SiO_2 bilayer in contrast reveals slightly decreased sensing response. The P3HT acts as the dominant charge transfer material in the P3HT–TiO_2 bilayer because it is much more conductive than TiO_2. The increase in sensing response of the device with an additional underlying TiO_2 nanorods layer suggests the TiO_2 layer might alter the surface properties and electronic properties of P3HT.

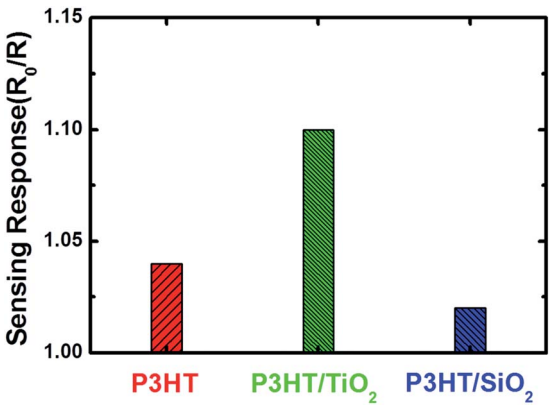

Fig. 4 Sensitivities of devices fabricated from the single layer P3HT film, the bilayer of P3HT–TiO_2 films and the bilayer of P3HT–SiO_2 films.

Thus, Kelvin probe force microscopy (KPFM) was utilized to in-depth investigate the oxygen sensing mechanism of P3HT–TiO_2 hybrid films. Fig. 5 shows the topographic images and surface potential images of pristine P3HT film and P3HT–TiO_2 hybrid films with various TiO_2 loading concentrations, 25 wt%, 50 wt% and 75 wt%. All the films were deposited by drop coating. The surface potential was found to decrease with increasing concentration of TiO_2 nanorods (Fig. 5). According to the work function difference between TiO_2 (~4.2 eV),[36,37] and P3HT (~5.0 eV, *cf.* Fig. 5(b)), the darker regions on the hybrid films (with smaller surface potential) are TiO_2-rich regions while the brighter regions are P3HT-rich region. Lower surface potential implies that electrons are easier to transfer to oxygen molecules and form the charge transfer complex, which results in higher sensing response. However, for the P3HT–TiO_2 hybrid film with 75 wt% TiO_2, larger P3HT and TiO_2 domain sizes can be observed in the surface potential mapping (Fig. 5(h)) as compared to that of 25% TiO_2 (Fig. 5(d)) and 50% TiO_2 (Fig. 5(f)). The pronounced phase separation would reduce the interface area and thus the electron donation between P3HT and TiO_2 which account for the decreased sensing responses.

The sensing response of the device is also dependent on the film thickness as shown in Fig. 6. Devices with different hybrid film thickness, *i.e.* 5.8 μm, 10.1 μm, and 13.4 μm, were made and evaluated for the oxygen sensing properties. The sensing response increases with the increase of hybrid film thickness (50 wt% TiO_2). The variation of the sensing response for the devices is believed due to the differences in morphology of the hybrid film. The thicker the film is, the more sites can be bound by oxygen molecule.

Furthermore, we made the device of hybrid film with 50 wt% TiO_2 nanorods annealed at 150 °C for 30, 60 and 120 minutes in

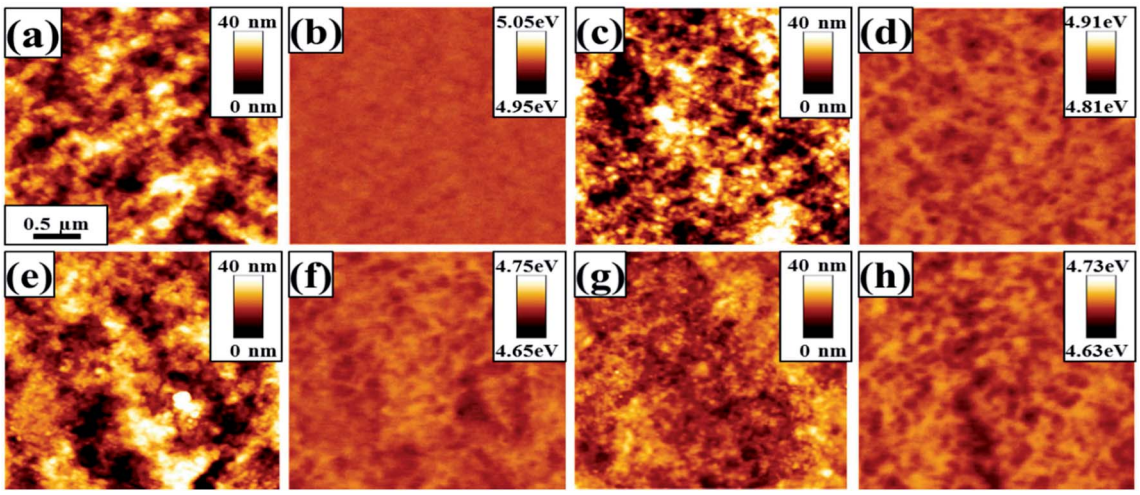

Fig. 5 KPFM images of pristine P3HT film (a and b) and P3HT–TiO_2 hybrid films with different TiO_2 concentrations (c and d) 25.0 wt%, (e and f) 50.0 wt%, and (g and h) 75.0 wt%. The (a, c, e and g) are topographic images and the (b, d, f and h) are corresponding surface potential images.

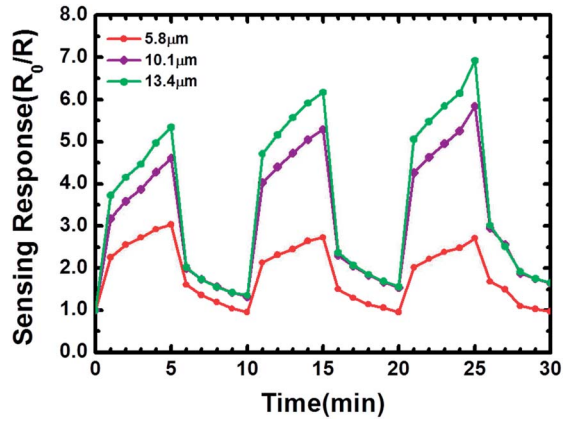

Fig. 6 Oxygen sensing response curve of drop cast P3HT–TiO_2 nanorods (1 : 1 composition) hybrid films of different thickness.

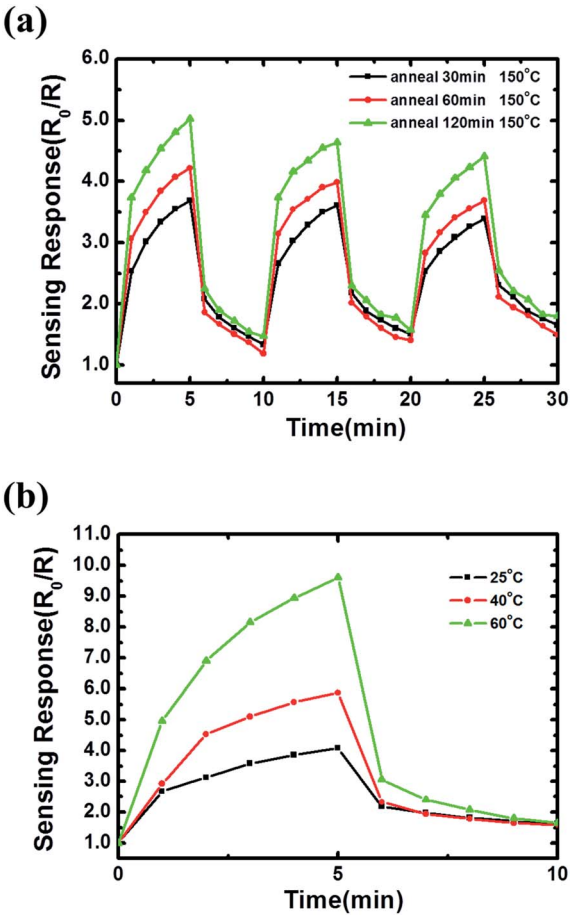

Fig. 7 (a) The sensitivities of 50 wt% TiO_2 nanorods hybrid films with different anneal time at 150 °C, and (b) the sensitivities of 50 wt% TiO_2 nanorods hybrid films at different testing temperature.

inert atmosphere (Fig. 7(a)). The sensing response is slightly increased with the increase of anneal time, which has been attributed to the removal of adsorbed oxygen molecules within the hybrid film. The characteristic of the oxygen sensing properties is not significantly changed for device annealed at 150 °C. Nevertheless, if the device of 50 wt% TiO_2 nanorods hybrid film which is annealed at 150 °C for 120 min is tested at 60 °C rather than room temperature, its sensing response can be increased by 3 times (Fig. 7(b)). Actually we have performed the oxygen sensing at higher temperature (over 100 °C). However, the devices as well as the testing chamber caught fire because of the high temperature and high concentration of oxygen. Therefore, in this study we only compared sensing performance between room temperature and heating at 40 °C and 60 °C (Fig. 7(b)) respectively. The sensing response increases with increasing testing temperature due to the accelerated adsorption and desorption of oxygen molecules.

Therefore, the employment of our sensor is expected to show good selectivity in ambient condition because of the inert characteristics of other components, *e.g.* N_2, Ar, *etc.* However, when being applied in other spaces such as factory or laboratory, it should be careful to the interruption resulted from other kinds of gases or organic vapors.

Conclusions

In this study, we demonstrate, by using the hybrid materials based on poly(3-hexyl thiophene) (P3HT) in combination with TiO_2 nanorods, improved oxygen sensing properties is obtained as compared to pristine P3HT. The result is attributed to the change of surface morphology and surface electronic properties of the hybrid film mandated by TiO_2. Moreover, we optimized the parameters of film thickness, annealing temperature and operating temperature. The results suggest that hybrid P3HT–TiO_2 nanorods is promising for resistive oxygen sensing at room temperature.

Acknowledgements

The authors are grateful to National Science Council of Taiwan for its financial support (Projects no. 102-2120-M-002-010 and 102-2633-E-182-001) and Chang Gung University Research Project.

References

1 M. Ogita, K. Higo, Y. Nakanishi and Y. Hatanaka, *Appl. Surf. Sci.*, 2001, **175–176**(1), 721–725.
2 W. J. Fleming, *J. Electrochem. Soc.*, 1977, **124**(1), 21–28.
3 R. K. Sharma, M. C. Bhatnagar and G. L. Sharma, *Sens. Actuators, B*, 1998, **46**(3), 194–201.
4 D. T. McQuade, A. E. Pullen and T. M. Swager, *Chem. Rev.*, 2000, **100**(7), 2537–2574.
5 V. C. Gonçalves, B. M. Nunes, D. T. Balogh and C. A. Olivati, *Phys. Status Solidi A*, 2010, **207**(7), 1756–1759.
6 M. S. A. Abdou, F. P. Orfino, Y. Son and S. Holdcroft, *J. Am. Chem. Soc.*, 1997, **119**(19), 4518–4524.
7 M. S. A. Abdou, F. P. Orfino, Z. W. Xie, M. J. Deen and S. Holdcroft, *Adv. Mater.*, 1994, **6**(11), 838–841.
8 G. M. Neelgund, V. N. Bliznyuk, A. A. Pud, K. Y. Fatyeyeva, E. Hrehorova and M. Joyce, *Polymer*, 2010, **51**(9), 2000–2006.

9 P. Schottlan, M. Bouguettaya and C. Chevrot, *Synth. Met.*, 1999, **102**(1–3), 1325.
10 B. Li, G. Sauvé, M. C. Iovu, M. Jeffries-El, R. Zhang, J. Cooper, S. Santhanam, L. Schultz, J. C. Revelli, A. G. Kusne, T. Kowalewski, J. L. Snyder, L. E. Weiss, G. K. Fedder, R. D. McCullough and D. N. Lambeth, *Nano Lett.*, 2006, **6**(8), 1598–1602.
11 H. C. Liao, C. P. Hsu, M. C. Wu, C. F. Lu and W. F. Su, *Anal. Chem.*, 2013, **85**(19), 9305–9311.
12 B. Li, S. Santhanam, L. Schultz, M. Jeffries-El, M. C. Iovu, G. Sauvé, J. Cooper, R. Zhang, J. C. Revelli, A. G. Kusne, J. L. Snyder, T. Kowalewski, L. E. Weiss, R. D. McCullough, G. K. Fedder and D. N. Lambeth, *Sens. Actuators, B*, 2007, **123**(2), 651–660.
13 H. H. Liao, C. M. Yang, C. C. Liu, S. F. Horng, H. F. Meng and J. T. Shy, *J. Appl. Phys.*, 2008, **103**(10), 104506.
14 V. Saxena, D. K. Aswal, M. Kaur, S. P. Koiry, S. K. Gupta, J. V. Yakhmi, R. J. Kshirsagar and S. K. Deshpande, *Appl. Phys. Lett.*, 2007, **90**(4), 043516.
15 J. H. He, C. H. Ho and C. Y. Chen, *Nanotechnology*, 2009, **20**(6), 065503.
16 A. S. Zuruzi, A. Kolmakov, N. C. MacDonald and M. Moskovits, *Appl. Phys. Lett.*, 2006, **88**(10), 102904.
17 J. A. Park, J. Moon, S. J. Lee, S. H. Kim, T. Zyung and H. Y. Chu, *Mater. Lett.*, 2010, **64**(3), 255–257.
18 L. Liao, H. B. Lu, J. C. Li, H. He, D. F. Wang, D. J. Fu, C. Liu and W. F. Zhang, *J. Phys. Chem.C*, 2007, **111**(5), 1900–1903.
19 Y. Hu, J. Zhou, P.-H. Yeh, Z. Li, T.-Y. Wei and Z. L. Wang, *Adv. Mater.*, 2010, **22**(30), 3327–3332.
20 J. Wu, G. Yue, Y. Xiao, J. Lin, M. Huang, Z. Lan, Q. Tang, Y. Huang, L. Fan, S. Yin and T. Sato, *Sci. Rep.*, 2013, **3**, 1283.
21 F. Li and X. Ni, *Sol. Energy Mater. Sol. Cells*, 2013, **118**, 109–115.
22 H. Li, J. Li, Q. Xu and X. Hu, *Anal. Chem.*, 2011, **83**(24), 9681–9686.
23 H. Geng, C. M. Hill, S. Pan and L. Huang, *Phys. Chem. Chem. Phys.*, 2013, **15**, 3504–3509.
24 M. C. Wu, H. C. Liao, Y. Chou, C. P. Hsu, W. C. Yen, C. M. Chuang, Y. Y. Lin, C. W. Chen, Y. F. Chen and W. F. Su, *J. Phys. Chem. B*, 2010, **114**(32), 10277–10284.
25 Y. T. Lin, T. W. Zeng, W. Z. Lai, C. W. Chen, Y. Y. Lin, Y. S. Chang and W. F. Su, *Nanotechnology*, 2006, **17**(23), 5781–5785.
26 T. W. Zeng, Y. Y. Lin, H. H. Lo, C. W. Chen, C. H. Chen, S. C. Liou, H. Y. Huang and W. F. Su, *Nanotechnology*, 2006, **17**(21), 5387–5392.
27 Y. Y. Lin, T. H. Chu, S. S. Li, C. H. Chuang, C. H. Chang, W. F. Su, C. P. Chang, M. W. Chu and C. W. Chen, *J. Am. Chem. Soc.*, 2009, **131**(10), 3644–3649.
28 Y. Y. Lin, T. H. Chu, C. W. Chen and W. F. Su, *Appl. Phys. Lett.*, 2008, **92**(05), 053312.
29 M. C. Wu, Y. J. Wu, W. C. Yen, H. H. Lo, C. F. Lin and W. F. Su, *Nanoscale*, 2010, **2**(8), 1448–1454.
30 R. P. Tandon, M. R. Tripathy, A. K. Arora and S. Hotchandani, *Sens. Actuators, B*, 2006, **114**(2), 768–773.
31 M. H. Seo, M. Yuasa, T. Kida, J. S. Huh, K. Shimanoe and N. Yamazoe, *Sens. Actuators, B*, 2009, **137**(2), 513–520.
32 J. A. Park, J. Moon, S. J. Lee, S. H. Kim, T. Zyung and H. Y. Chu, *Mater. Lett.*, 2010, **64**(3), 255–257.
33 A. Ruiz, J. Arbiol, A. Cirera, A. Cornet and J. R. Morante, *Mater. Sci. Eng., C*, 2002, **19**(1–2), 105–109.
34 F. Kong, Y. Wang, J. Zhang, H. Xia, B. Zhu, Y. Wang, S. Wang and S. Wu, *J. Mater. Sci. Eng. B*, 2008, **150**(1), 6–11.
35 D. J. Yang, I. Kamienchick, D. Y. Youn, A. Rothschild and I. D. Kim, *Adv. Funct. Mater.*, 2010, **20**(24), 4258–4264.
36 T. T. Y. Tan, C. K. Yip, D. Beydoun and R. Amal, *Chem. Eng. J.*, 2003, **95**(1–3), 179–186.
37 A. J. Breeze, Z. Schlesinger and S. A. Carter, *Phys. Rev. B: Condens. Matter Mater. Phys.*, 2001, **64**(12), 125205.

